

Multifunctional Nanoassemblies for Cytotoxic Drug and Therapeutic Enzymes Delivery in Neuroblastoma Therapy

Jorge Parra-Nieto, María Amor García del Cid, Carolina Galeano, Iñigo Aguirre de Carcer, Lorena García-García, África Gonzalez-Murillo, Diego Megias, Manuel Ramirez, and Alejandro Baeza*

Neuroblastoma cells can acquire resistance mechanisms that make them invulnerable to chemotherapeutic agents. The use of nanoparticles as drug carriers provides the possibility to deliver several drugs simultaneously to specific tumoral cell populations, improving their therapeutic outcome. Herein, the development of a multifunctional nanoplatform based on the assembly of protocells (PC) and polymeric nanocapsules (PNC) is reported. PC provides the ability to transport and release cytotoxic drugs while PNC offers the capacity to transport enzymes to the tumoral tissues preserving their catalytic activity. Doxorubicin (Dox) and Glucose Oxidase (Gox) are housed within PC and PNC, respectively. The external surface of these nanoassemblies is decorated with synthetic targeting moieties, providing selectivity to neuroblastoma cells. Thus, the nanoplatform is endowed with the ability to generate multiple insults within neuroblastoma cells as cytotoxic drug release, glucose starvation, and oxidative damage. This nanoplatform exhibits significantly higher cytotoxic activity in comparison with only drug-loaded protocells or empty protocells decorated with glucose oxidase nanocapsules, which points out the existence of a potent synergic effect between the action of both therapeutic agents: Dox and Gox. This strategy can be adapted to the production of multifunctional nanoassemblies, improving the arsenal against different types of tumors.

1. Introduction

Neuroblastoma (NB) corresponds to 15% of infant cancer mortality being the most frequent extracranial tumor in children.^[1] The current treatment of this disease is based on the combination of chemo- and radiotherapy, surgical resection, and immunotherapy, but the prognosis of NB in metastatic stages is still poor, showing a survival rate lower than 40%.^[2] In addition, chemotherapeutic drugs are usually employed at high dosages which leads to long-term toxicity.^[3] Therefore, novel therapeutic strategies which improve the survival rate and life quality of the patients are urgently needed. During the last decades, the use of nanoparticles as drug carriers has emerged as a powerful approach to deliver therapeutic agents into tumoral tissues in a selective and controlled manner.^[4–6] Nano-sized carriers tend to be accumulated in tumoral tissues by the well-known enhanced permeation and retention (EPR) effect.^[7] This effect exploits the aberrant tumoral blood vessel architecture

characterized by the presence of large pores and fenestrations in the vessel wall which allows the extravasation of nanoparticles in the malignancy. Furthermore, the lack of a functional lymphatic system in the solid tumors compromises the drainage of the nanocarrier out of the diseased tissue inducing its accumulation during long periods of time. Even though the role of this effect in human cancers has been the subject of controversy in the last years,^[8] different strategies have been recently reported to enhance the nanoparticle accumulation in tumors either through pharmacological strategies to modulate the tumor blood flow and/or the vasculature,^[9] as well as through the modification of the tumoral stroma.^[10] In any case, the accumulation of nanocarriers in the tumoral tissue in many cases would be not enough to guarantee an efficient therapeutic response.^[11] Nanocarriers should be endowed with the capacity to recognize their target cell within the myriad of different cell populations that usually populate a solid tumor.^[12] Our research group reported the use of aminobenzylguanidines moieties (ABG) as targeting agents capable to induce a significant in vivo accumulation of

J. Parra-Nieto, M. A. García del Cid, C. Galeano, I. A. de Carcer, A. Baeza
Dpto. Materiales y Producción Aeroespacial
ETSI Aeronáutica y del Espacio
Universidad Politécnica de Madrid
Madrid 28040, Spain
E-mail: alejandro.baeza@upm.es

L. García-García, A. Gonzalez-Murillo, M. Ramirez
Servicio de Hematología y Oncología Pediátrica
Hospital Infantil Universitario Niño Jesús
Madrid 28009, Spain

D. Megias
Advanced Optical Microscopy unit
Instituto de salud Carlos III (ISCIII)
Madrid 28222, Spain

 The ORCID identification number(s) for the author(s) of this article can be found under <https://doi.org/10.1002/admi.202201356>.

© 2022 The Authors. Advanced Materials Interfaces published by Wiley-VCH GmbH. This is an open access article under the terms of the Creative Commons Attribution License, which permits use, distribution and reproduction in any medium, provided the original work is properly cited.

DOI: 10.1002/admi.202201356

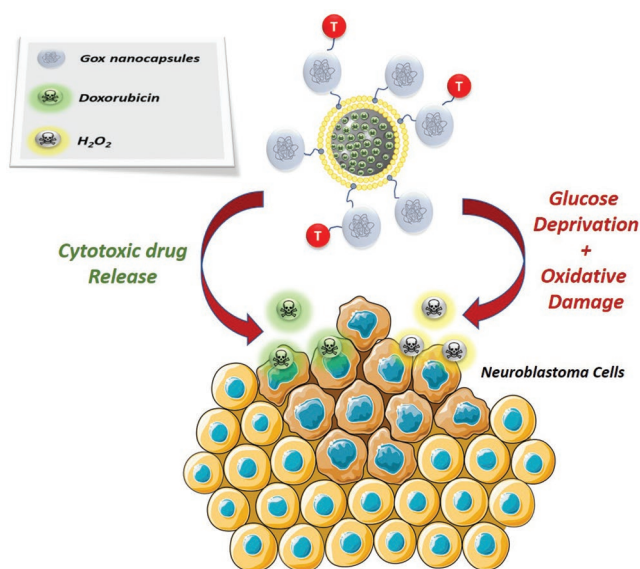


Figure 1. Mechanism of action of targeted multifunctional nanoassemblies: cytotoxic drug release in combination with glucose depletion and oxidative damage by the action of Gox_{nc} .

nanocarriers in neuroblastoma tissues.^[13,14] These analogues exhibit strong affinity to norepinephrine transporter (NET), a cell membrane receptor overexpressed by more than 90% of neuroblastoma cells.^[15] The apparition of multidrug resistance (MDR) is associated with $\approx 90\%$ of mortality in cancer patients.^[16] Nanoparticles can be engineered to deliver therapeutic cocktails in a controlled manner overwhelming the MDR-associated mechanisms of the tumoral cells.^[17] Protocells (PC) are formed by an inorganic core of mesoporous silica, which can be loaded with high amount of different drugs, coated with a lipid bilayer that avoids their premature release.^[18] This nanodevice combines the outstanding loading capacity of mesoporous silica nanoparticles with the excellent biocompatibility and colloidal stability of liposomes. An important advantage of these nanocarriers is that the protocells release their payload once they enter the target cell due to the endosomal acidic environment which destabilizes the lipid bilayer.^[19] Therefore, the design of usually complex stimuli-responsive drug release mechanism is not required. In addition, the lipid composition of the liposome coating can be easily tuned to incorporate functional groups which allows the attachment of targeting moieties^[20] and even other nanoparticles.^[21] This property allows the possibility to engineer nanoassemblies composed by different nanoparticles to combine their effects achieving unique synergic effects. Herein, we report the synthesis and biological evaluation of a novel nanoplatform composed by protocells decorated with specific targeting moieties to neuroblastoma cells and glucose oxidase nanocapsules (Gox_{nc}). Glucose oxidase (Gox) is an oxido-reductase that catalyzes the oxidation of glucose into gluconic acid and H_2O_2 in the presence of O_2 . The use of this enzyme in antitumoral therapy has been addressed in the last decades due to its capacity to induce starvation in tumoral cell by intratumoral glucose consumption and oxidative damage provoked by H_2O_2 .^[22] In our nanoplatform, Gox

was encapsulated within polyacrylamide-based nanocapsules to protect its catalytic function in physiological environments where proteolytic enzymes among other harsh conditions are present. These polymeric nanocapsules have proven their capacity to maintain the function of the housed enzymes against several insults as high concentrations of proteases or high temperatures.^[23,24] The mesoporous silica core of these protocells was loaded with a potent cytotoxic drug, doxorubicin (Dox). The presence of the targeting moieties on the protocell surface enhanced the uptake of the nanoplatform in neuroblastoma cells and once inside them, the combined action of Dox release, glucose depletion, and H_2O_2 production induced a substantial tumoral cell viability decrease at low dosages ($1.5 \mu g mL^{-1}$) (Figure 1). The antitumoral capacity of this nanoplatform was significantly higher to the results gathered with simply drug-loaded protocells and protocells only endowed with glucose oxidase nanocapsules, which pointed out the existence of a potent synergic effect between Dox and Gox action. Moreover, the presence of targeting moieties on the nanoplatform surface allowed the enhanced uptake in neuroblastoma cells allowing the use of low doses which were non-toxic to healthy cells.

2. Results and Discussion

2.1. Synthesis of Protocells

Mesoporous silica nanoparticles (MSN) with hexagonally arranged pore network and pore diameter between 3 and 4 nm was synthesized as PC core due to its proven efficacy to house chemotherapeutic agents.^[25] MSN was synthesized following a methodology previously reported^[21] harvesting MSN with an average diameter of 150 nm according to dynamic light scattering (DLS) (Figure S2, Supporting Information) measurements and transmission electron microscopy (TEM) (Figure 2a). In order to allow the evaluation of nanoparticle cell uptake by fluorescence microscopy and flow cytometry, MSN were covalently labelled with fluorescein.

For lipid bilayer coating, two types of liposomes which carried amino or carboxylic groups on their surface were synthesized through thin film hydration method^[26] employing 1,2-distearoyl-sn-glycero-3-phosphoethanolamine-N-[amino(polyethylene glycol)-2000] (DSPE-PEG(2000)- NH_2) and 1,2-distearoyl-sn-glycero-3-phosphoethanolamine-N-[carboxy(polyethylene glycol)-2000] (DSPE-PEG(2000)-COOH), respectively, in combination with 1,3-distearoyl-sn-glycero-3-phosphocholine (DSPC) and cholesterol. According to our previous work,^[21] 15% of functional groups were enough to allow an efficient surface attachment of nanoparticles or targeting moieties. The effect of the lipid composition in the stability, chemical structure, and capacity to form protocells of the liposomes was widely studied by Brinker et al.^[18–20] In our work, liposomes were synthesized employing a fixed ratio of DSPC/Cholesterol/DSPE-PEG(2000)- NH_2 (or COOH) (65:20:15), a composition which was found optimal in a previous work carried out by our research group.^[21] The obtained liposomes were extruded through a 100 nm polycarbonate membrane to provide liposomes with a narrow distribution of sizes around 90 nm.

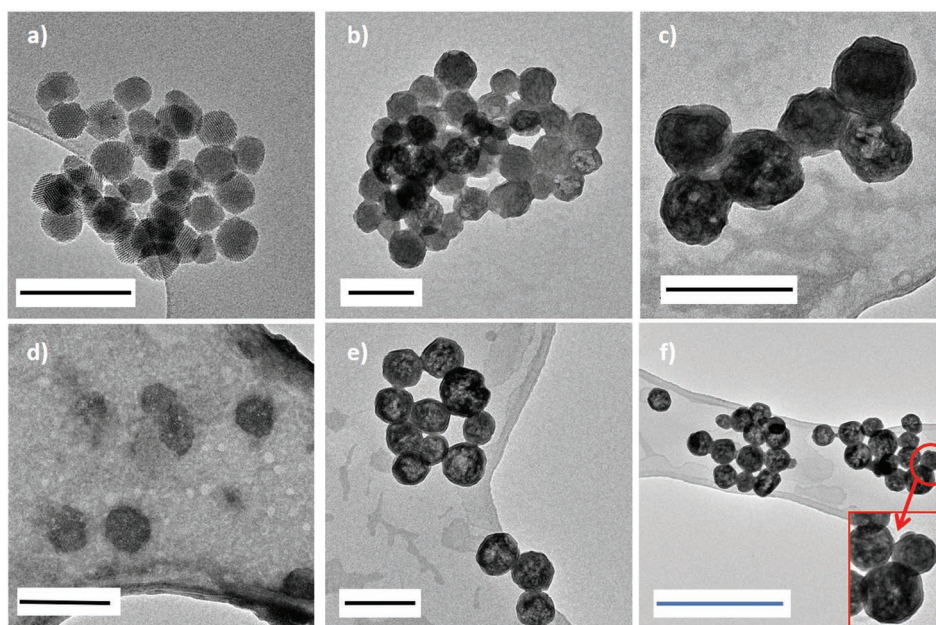
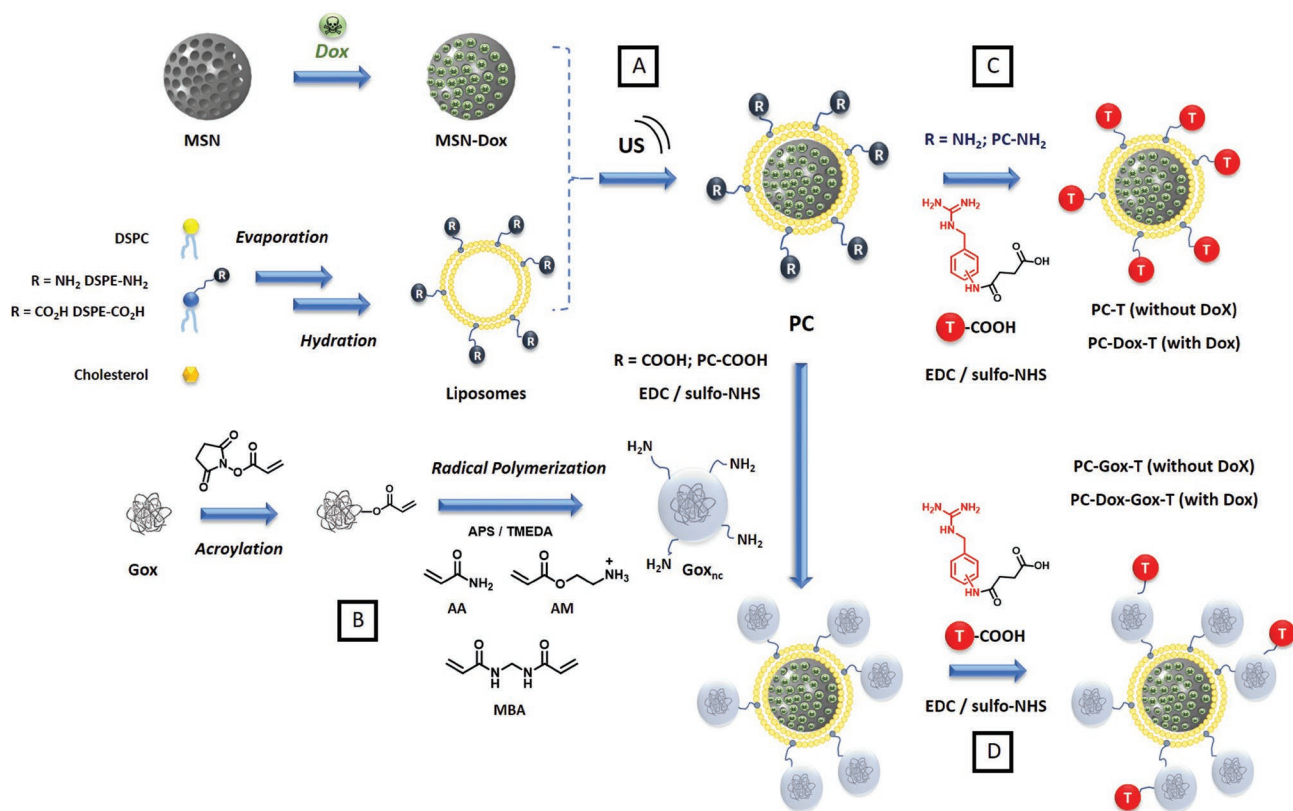


Figure 2. TEM images of a) MSN, b) PC-NH₂, c) PC-T, d) Gox_{nc}, e) PC-COOH, and f) PC-Gox_{nc}-T. Black bars correspond to 200 nm and blue bar corresponds to 500 nm. Samples (b–f) were stained with phosphotungstic acid to improve the contrast. Red boxed image shows Gox_{nc} on protocol cell surface. Additional TEM images of these nanoparticles and elemental analysis by EDX are shown in Figure S1, Supporting Information.

Protocells were synthesized by ultrasound-assisted fusion of liposomes with MSN (Scheme 1A). MSN were mixed with their respective liposomes (functionalized with amino or carboxylic

groups, respectively) in phosphate buffered saline (PBS at pH 7.2) under strong sonication for 30 s. The protocell formation was ruled out by the spontaneous fusion between the liposomes



Scheme 1. Synthetic pathway of A) PC, B) Gox_{nc} and PC-Gox_{nc}, C) PC-T, and D) PC-Gox_{nc}-T.

and mesoporous silica nanoparticles due to the highly lipophilic nature of the silica surface.^[27] This methodology yielded PC-NH₂ or PC-COOH, depending on the functional group present on the precursor liposomes. Protocells were characterized by TEM employing phosphotungstic acid as electron opaque contrast agent to allow the visualization of the thin lipid coating (Figure 2b,e). As it is shown in these micrographs, the particle sizes were centered around 150–180 nm, which agreed with DLS measurements (Figure S2, Supporting Information). Elemental analysis of the protocell surface by Energy Dispersive X-Ray (EDX) showed a higher amount of phosphorous in the protocells in comparison with naked mesoporous silica nanoparticles which confirmed the existence of lipid bilayer on MSN surface (Figure S1, Supporting Information). The as-synthesized protocells present different functional groups on their surface to allow the further attachment of targeting moieties and glucose oxidase nanocapsules, and polyethylene chains (PEG). The presence of PEG hampers the opsonization process, a prerequisite for macrophage capture of foreign bodies, and therefore, increases the circulation time of the nanocarriers within the host.^[28] In addition, it has been described that the colloidal stability of PEGylated nanocarriers is usually higher than naked nanoparticles because these polymeric chains difficult the nanoparticle aggregation by steric hindrance.^[29] Zeta potential measurements confirmed the incorporation of a lipid bilayer on the MSN surface. Naked MSN showed a Zeta potential in aqueous solution of −7.1 mV (Figure S3, Supporting Information). The fusion of MSN with liposomes decorated with amino groups (Zeta potential +4.8 mV) yielded protocells (PC-NH₂) with a surface charge around +4.3 mV which confirms the presence of the lipid bilayer on their surface. In the case of the formation of protocells decorated with carboxylic groups (PC-COOH), a slight increase in the negative charge on the surface was observed (Zeta potential −9.5 mV), confirming the incorporation of the lipid bilayer endowed with carboxylate groups on the nanoparticle surface (Figure S3, Supporting Information).

2.2. Synthesis of Gox Nanocapsules

Due to the labile nature of enzymes, their use in therapeutic applications is usually hampered by the harsh conditions present in living tissues, as is the case of proteolytic enzymes and oxidative agents, among others, which induce a significant reduction in the lifetime and catalytic activity of these biomolecules.^[30] The encapsulation of proteins and enzymes into protective nanocarriers has emerged as a valuable strategy to deliver these sensible macromolecules to diseased tissues.^[31] Among the different enzyme encapsulation strategies, the use of polymeric nanocapsules presents important advantages as their low Young modulus which facilitates extravasation, circulation time, and tissue penetration^[32] or their high tuneability, that allows the incorporation of multiple functional groups and stimuli-responsive moieties.^[33] Our research group has described the synthesis of polymeric nanocapsules capable to load different enzymes as horse radish peroxidase,^[34] catalase^[23] or collagenase^[24] keeping their catalytic activity even in the presence of high temperature and high concentration

of proteases. Furthermore, in previous works, these nanocapsules were designed to present tunable pH-responsive behavior being able to release their payload on demand depending on the pH present in the tissue.^[35] Herein, glucose oxidase has been encapsulated into non-degradable polyacrylamide-based nanocapsules formed by radical polymerization using acrylamide (AA) as structural monomer, 2-aminoethylmethacrylate (AM) to provide functional groups that allows the further attachment of the nanocapsules on the protocell surface, and *N,N'*-methylenebis(acrylamide) (MBA) as crosslinker. Previous to the nanocapsule formation, Gox was decorated with acryloyl groups to introduce polymerizable groups on the enzyme surface. This step was carried out through the addition of *N*-acryloxysuccinimide to an aqueous solution of Gox at pH 8.5, in order to enhance the nucleophilic behavior of the amino groups present in the protein. Then, the polymer nanocapsules were synthesized around acryloylated Gox by radical polymerization employing a monomer ratio of AA:AM:MBA (12:9:1) and enzyme:monomer ratio of 1:1400 in the presence of ammonium persulphate/*N,N,N',N'*-tetramethyl ethylenediamine (APS/TMEDA) as radical initiator mixture (Scheme 1B). Gox nanocapsules were characterized by DLS and TEM showing a round-shaped morphology and average size diameter around 80 nm. Zeta potential of Gox_{nc} was determined in aqueous surface showing a value around +3.5 mV. The catalytic activity of the encapsulated enzyme was determined employing a commercial kit (enzymatic assay of glucose oxidase, Merck) based on the catalytic oxidation of *o*-dianisidine by the hydrogen peroxide released by Gox in the presence of glucose and peroxidase. Free Gox presents an enzymatic activity of 60 U mg^{−1} of solid while Gox_{nc} exhibited 14.8 U mg^{−1} of solid (Figure 3). This reduction in the catalytic activity can be attributed to protein denaturalization during the purification steps and also to the diffusion barrier created by the polymer coating. The loss of enzymatic activity is compensated by the improved resistance provided by the polymeric nanocapsules. The enzymatic activity of a solution of Gox_{nc} kept in the fridge is retained during long periods of times (up to 1 month) whereas a solution of free Gox kept in the same conditions lost its catalytic activity in a few days. The protective role of these polymeric coatings agrees with the results observed with other enzymes.^[23,24]

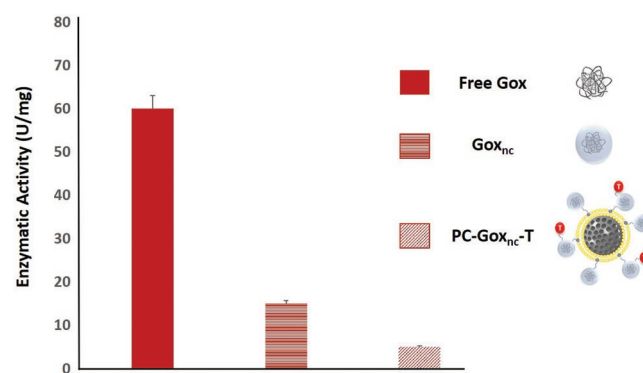


Figure 3. Enzymatic activity of free Gox, Gox_{nc}, and PC-Gox_{nc}-T. All experiments were performed in triplicate.

2.3. Evaluation of the Nanoparticle Uptake of Targeted Protocells in NB Cells

The use of nanocarriers to deliver therapeutic agents to specific cell populations requires the incorporation of targeting moieties on their surface. These targeting groups can be small molecules as vitamins, sugars or synthetic molecules or large macromolecules such as antibodies, proteins or oligonucleotides.^[12] As it has been mentioned above, our research group reported that aminobenzylguanidine (ABG) analogues can be anchored on the surface of nanoparticles to induce their selective accumulation into neuroblastoma cells due to their high binding affinity by norepinephrine transporter protein usually overexpressed by these tumoral cells.^[13,14] In this work, meta-aminobenzylguanidine (mABG) and para-aminobenzylguanidine (pABG) functionalized with a terminal carboxylic group were anchored on the surface of fluorescein-labeled protocells in order to evaluate their capacity to enhance the accumulation of these nanocarriers into NB cells. These targeting analogues were covalently grafted on the surface of protocell decorated with amino groups (PC-NH₂) employing carbodiimide chemistry yielding the corresponding targeted protocells (PC-T) (Scheme 1C). A fixed concentration of Protocells (75 μg mL⁻¹) functionalized with m-ABG (PC-mABG) or p-ABG (PC-pABG), respectively, were incubated with two different neuroblastoma cell lines (NB1691 and LAN-1) for 2 h. After this time, cells were thoroughly washed to remove the excess of protocells and then, cells were incubated for 24 h more. The percentage of cells which contained nanoparticles was measured by flow cytometry. The results showed that protocells functionalized with m-ABG (PC-mABG) barely enhanced the uptake in both cell lines in comparison with protocells without targeting (12% in comparison with 5% of the non-targeted protocells). The cellular nanoparticle uptake in the case of protocells functionalized with p-ABG (PC-pABG) was significantly higher in both cell lines inducing up to fivefold higher uptake than PC-mABG and more than tenfold higher than PC without targeting (Figure 4a).

These excellent results confirmed that pABG is an excellent targeting moiety for neuroblastoma therapy and this analogue was selected as targeting group in further experiments.

In order to confirm that protocells were truly engulfed within the tumoral cells, NB1691 cells were incubated with the same concentration of PC-pABG for 24 h and after this time, the localization of the nanoparticles was determined by confocal fluorescence microscopy. The cell nuclei were stained with DAPI (blue) and cell cytoplasm were stained with HCS CellMask Deep Red Stain (red). The confocal images showed that a significative fraction of nanocarriers was able to reach the inner cellular space, as can be observed by the existence of perinuclear green dots which correspond to the FITC covalently grafted on MSN cores of the protocells (Figure 5; Video S1, Supporting Information).

2.4. Attachment of Gox_{nc} and Targeting Moieties on Protocell Surface

Free amino groups present on the surface of Gox_{nc} were employed as anchoring points of Gox_{nc} on protocell surface provided with carboxylic groups (PC-COOH). Thus, PC-COOH were incubated with *N*-(3-dimethylaminopropyl)-*N*'-ethylcarbodiimide hydrochloride (EDC) and *N*-hydroxysulfosuccinimide sodium salt (sulfo-NHS) in PBS (pH 7.2) during 30 min. After this time, protocells were thoroughly washed to remove the excess of reagents. Then, they were suspended in PBS (pH 7.2) and a solution of Gox_{nc} was added. The mixture was gently shaken for 24 h to allow the amide bond formation between the activated carboxylic groups present on protocells and the amino groups of Gox_{nc}. PC-Gox_{nc} was characterized by DLS showing a homogeneous size distribution centered around 200–250 nm, which agrees with the size increment caused by the attachment of Gox_{nc} on the protocell surface. In addition, the surface charge changed from -9.5 to -5.8 mV (Figure S3, Supporting Information) which confirmed the incorporation of

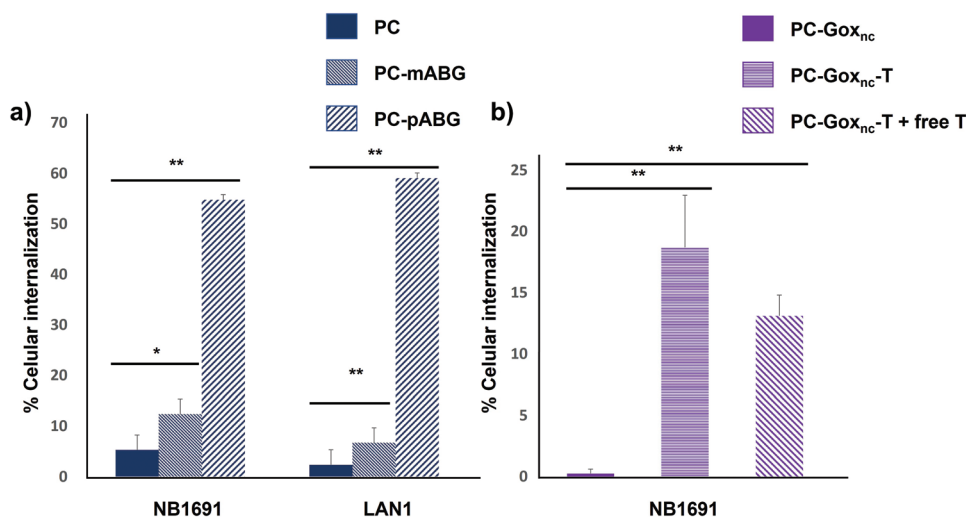


Figure 4. In vitro nanocarrier uptake evaluation in neuroblastoma cells of a) protocells with ABG analogues incubated in NB1691 and LAN1 cell lines, and b) PC-Gox_{nc} functionalized with and without p-ABG in NB1691 cell line. All experiments were performed in triplicate, * = $p < 0.01$, ** = $p < 0.05$. Flow cytometry analysis is shown in Figures S4 and S5, Supporting Information.

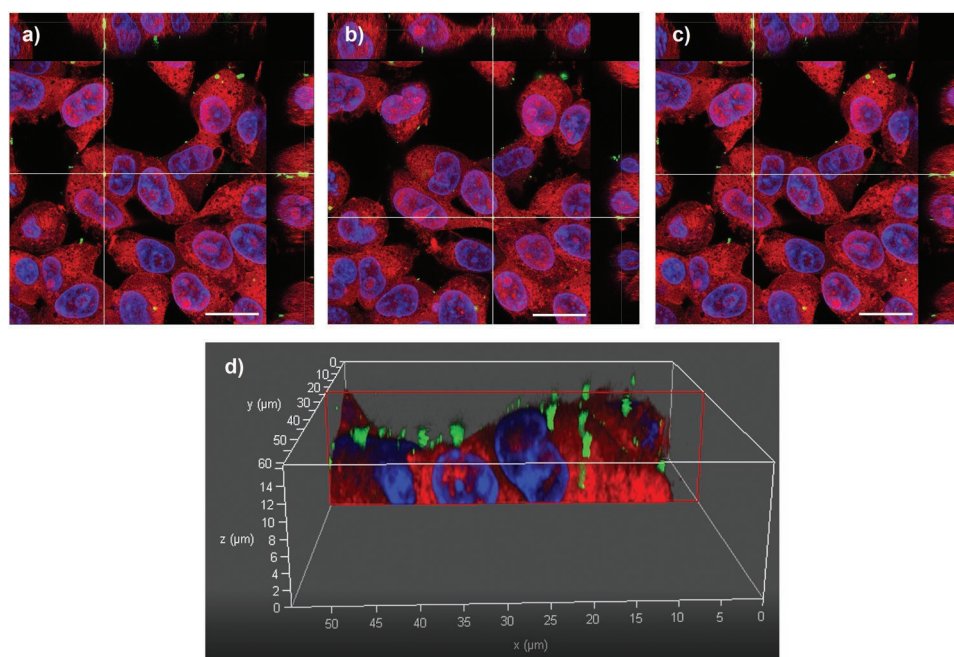


Figure 5. Images a–c) Evaluation of nanoparticle uptake of PC-pABG by confocal fluorescence microscopy in NB cells. Cell nuclei are stained in blue; cell cytoplasm was stained in red using HCS CellMask Deep Red Stain, and protocells were labeled in green (white bars correspond to 25 μm). The bottom and side panels show the x–z and y–z cross-sectional images, respectively. Image d) 3D snapshot of video provided in Video S1, Supporting Information. Other video file of a different zone is provided in Video S2, Supporting Information.

positively charged nanocapsules on the protocell surface. Furthermore, the presence of Gox_{nc} was proved by TEM employing phosphotungstic acid as staining agent to allow the visualization of organic materials by electron microscopy (Figure 2f). The presence of active Gox_{nc} on the protocells was confirmed measuring the enzymatic activity of the encapsulated enzyme covalently attached on PC- Gox_{nc} , which indicated that PC- Gox_{nc} presented significantly high enzymatic activity (Figure 3).

Finally, pABG moieties were covalently anchored to PC- Gox_{nc} by carbodiimide chemistry with the free amino groups present on Gox_{nc} and carboxylic groups of the targeting analogues yielding the corresponding targeted nanocarriers PC- $\text{Gox}_{\text{nc}}\text{-T}$ (Scheme 1D). Once the targeting moieties were attached on the nanocarrier surface, nanoparticle uptake by neuroblastoma cells was evaluated. In this case, only the NB1691 cell line was employed, due to the similar behavior between both neuroblastoma cell lines observed in previous targeting evaluation studies. NB cells were incubated with a fixed amount of PC- $\text{Gox}_{\text{nc}}\text{-T}$ suspended in PBS ($70 \mu\text{g mL}^{-1}$) for 2 h. After this time, cells were thoroughly washed to remove the excess of protocells and they were incubated 24 h more. The results indicated that PC- $\text{Gox}_{\text{nc}}\text{-T}$ exhibited a drastically higher cellular uptake in comparison with non-targeted nanocarriers (PC- Gox_{nc}), (18% vs 0.3%, respectively) (Figure 4b). In this case, the percentage of cells which engulfed PC- $\text{Gox}_{\text{nc}}\text{-T}$ was lower than the percentage of cells with PC-T (18% vs 55%, respectively). The reason of this difference could be attributed to the lower amount of targeting moieties which can be anchored in each system. In the case of PC-T, the amount of free amino groups on which the targeting moiety can be covalently grafted are higher than the free amino groups present on the nanocapsule surface in PC- $\text{Gox}_{\text{nc}}\text{-T}$.

Therefore, the amount of attached targeting groups in the last system should be lower. In any case, the targeting effect is even superior in the case of PC- $\text{Gox}\text{-T}$ inducing 50-times higher nanoparticle uptake in neuroblastoma cells than the non-targeted system. To evaluate if the enhanced uptake is induced by receptor-mediated endocytosis, a competitive experiment was carried out. In this case, neuroblastoma cells were incubated with PC- $\text{Gox}_{\text{nc}}\text{-T}$ in a medium with high concentration of free pABG ($35 \mu\text{M}$). This presence of free targeting groups induced a significant reduction in the cellular uptake of more than 30%, which confirmed the existence of active nanoparticle endocytosis mediated by NET receptors (Figure 4b).

2.5. Evaluation of Cytotoxic Capacity of Drug-loaded PC-T and PC- $\text{Gox}_{\text{nc}}\text{-T}$ in Neuroblastoma Cells

As it has been mentioned in the introduction, Protocells constitute an interesting platform to deliver therapeutic agents to tumoral tissues due to the excellent loading capacity provided by the mesoporous silica core. In our system, PC- $\text{Gox}_{\text{nc}}\text{-T}$ can combine the ability to transport chemotherapeutic agents with the own cytotoxic activity of Gox , providing a potent synergic effect to selectively eliminate the neuroblastoma cells. In order to evaluate this capacity, protocells were loaded with a potent cytotoxic drug widely employed in antitumoral therapy as is Dox.^[36] Thus, previous to the liposomal fusion step in the protocell synthetic pathway, mesoporous silica nanoparticles were soaked into an aqueous solution of doxorubicin (5 mg mL^{-1}) during 24 h. The amount of doxorubicin trapped within the silica network was estimated by UV/VIS

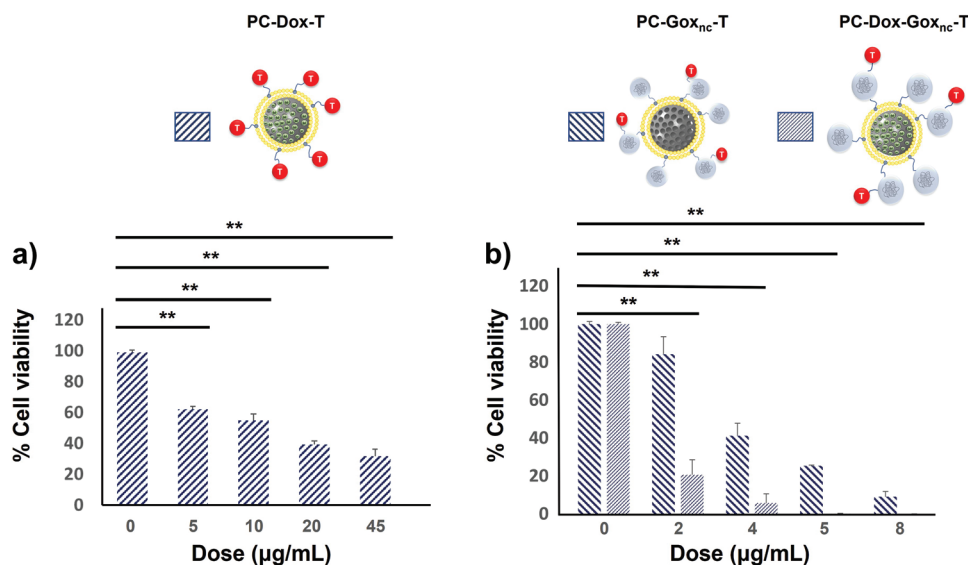


Figure 6. Cell viability studies with NB1691 cells incubated with the respective nanocarrier dosages for 24 h of a) PC-Dox-T and b) PC-Gox_{nc}-T and PC-Dox-Gox_{nc}-T. All experiments were performed in triplicate, ** = $p < 0.05$. Flow cytometry analysis is shown in Figures S7 and S8, Supporting Information.

spectroscopy at 490 nm by comparison between the concentration of doxorubicin in the initial aqueous solution with the supernatant once the mesoporous silica nanoparticles were removed. The results indicated that mesoporous silica nanoparticles presented a loading capacity of 6% w/w and loading efficiency of 34% (applying the equation Dox loading efficiency = $[(W_{\text{Dox gross}} - W_{\text{Dox supernatant}}) / W_{\text{Dox gross}}] \cdot 100$). Dox-loaded protocells were employed for the synthesis of PC-Dox-T and PC-Dox-Gox_{nc}-T following the same methodology mentioned for the empty systems. The Dox release behavior was studied both in naked mesoporous silica nanoparticles and in protocells, at two different pH conditions: physiological environment (pH 7) and slightly acidic conditions (pH 5.5). The mild acidic media mimics the conditions present in many solid tumors, and the acidic environment present in late endosomes and lysosomes.^[37] The results showed that Dox release exhibited by naked MSN was significantly accelerated in mild acidic environment in comparison with physiological conditions (Figure S6, Supporting Information). The reason for this behavior could be the change in the surface charge in this condition, which becomes less negative reducing its capacity to retain Dox. Protocells did not exhibit significant Dox release in both pH, which confirmed the protective role of the lipid coating which hampered the premature release of the Dox housed within the silica network. The addition of an aqueous media enriched with a surfactant CATB (10%), induced the distortion of the lipidic bilayer provoking the Dox departure. These results supported the controlled release behavior of the protocells, which avoided the premature departure of the housed drugs until the lipid bilayer was detached, which would happen when the nano-system entered the target cell.

Once PC-Dox-T and PC-Dox-Gox_{nc}-T were synthesized, their cytotoxic capacity was evaluated in neuroblastoma cell line (NB1691) through both dose-response assays. Thus, cells were incubated for 24 h at 37 °C and 5% CO₂ atmospheric concentration with increasing concentrations of the respective protocells

and then, cell viability was determined by flow cytometry employing 7-Amino Actinomycin D (7AAD) to differentiate dead or alive cells. The results showed significant differences in the cytotoxicity between both systems. PC-Dox-T required dosages at 20 µg mL⁻¹, to reduce the cell viability more than 50% while empty protocells decorated with Gox_{nc} (PC-Gox_{nc}-T) were capable to induce similar cell viability reduction with five-times lower dosage (Figure 6). Interestingly, when the protocells were endowed with both therapeutic agents, Gox_{nc} and Dox, extremely low dosages of 2 µg mL⁻¹ provoked more than 80% of cell mortality, which confirmed the synergic effect of the catalytic action of Gox with low concentrations of Dox.

Finally, in order to evaluate the cytotoxicity of these protocells in healthy cells, human mesenchymal cells (MSC) were employed as cellular model which do not overexpress NET receptors. MSC and NB1691 cells were incubated during 2 h with a high concentrated solution of PC-Dox-T and PC-Dox-Gox_{nc}-T (70 µg mL⁻¹). After this time, the cells were thoroughly washed, and they were incubated during 24 h more to evaluate the toxicity provoked by the engulfed protocells. The results indicated that PC-Dox-Gox_{nc}-T barely affect the cell viability of MSC whereas it induced a strong cytotoxicity in NB1691 cells (around 60% of cell viability reduction) (Figure 7a). In addition, nanoparticle uptake in each cell population was evaluated by fluorescence microscopy using the fluorescein covalently attached on the mesoporous silica network (excitation and emission wavelengths of 488 and 525 nm, respectively) and the own fluorescence of doxorubicin, which presented maximum emission wavelength close to 600 nm.^[38] Fluorescence microscopy images showed that MSC did not present fluorescence in both fluorescein and doxorubicin channels, which confirmed the lack of protocell uptake in these cells (Figure 7b). The scarce nanoparticle uptake exhibited by these cells would explain the lack of toxicity observed in this case. In the case of NB1691 cells, they exhibited multiple green fluorescence dots and extended red fluorescence along the cells that indicated that

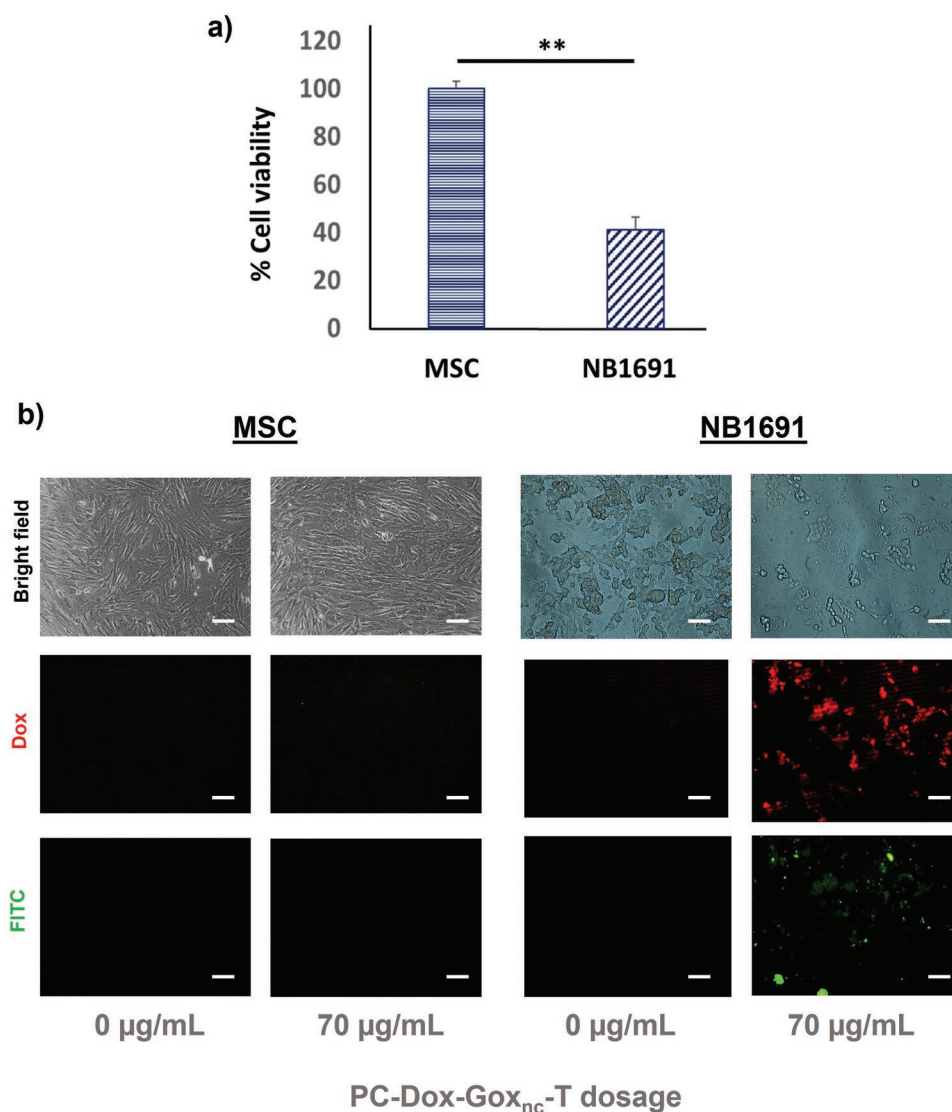


Figure 7. a) Cell viability evaluation of MSC and NB1691 cells incubated with PC-Dox-Gox_{nc}-T. All experiments were performed in triplicate, ** = $p < 0.05$. Flow cytometry analysis is shown in Figure S9, Supporting Information. b) Fluorescence microscopy images of MSC and NB1691 cells incubated with and without PC-Dox-Gox_{nc}-T. Green dots shown in FITC channel correspond to fluorescein-labeled MSN and red dots corresponds to Dox. Scale bar corresponds to 25 µm.

nanoparticles were engulfed, and the loaded Dox was released in the inner cellular space causing their elimination.

These results confirmed the excellent behavior of these multifunctional nanoassemblies which were capable to be efficiently engulfed by neuroblastoma cells and once there, perform a synergistic action. This was, on the one hand, to release the cytotoxic drugs housed within the mesoporous silica core and on the other hand, to generate radical oxidative species and glucose deprivation enhancing the therapeutic efficacy of these nanoassemblies.

3. Conclusion

In this work, a novel nanoplatform able to deliver different therapeutic agents to neuroblastoma cells has been reported.

This nanoplatform is based on the covalent assembly of proto-cells and polymeric nanocapsules. These nanoassemblies combine the high loading capacity of the mesoporous silica core, which can be used to house multiple chemotherapeutic agents, the excellent colloidal stability and biocompatibility of the liposomal coating, and the versatility of the polymer nanocapsules, that can be engineered to deliver sensitive macromolecules to tumoral tissues. Herein, two therapeutic agents have been employed as drug models, doxorubicin and glucose oxidase, showing significant synergic antitumoral efficacy in neuroblastoma cells. The selectivity has been provided by the incorporation of aminobenzylguanidine analogues on the nanoplatform surface, a family of analogues with proven capacity to guide nanocarriers to neuroblastoma tumors. These nanoassemblies have showed improved uptake and substantial cytotoxic capacity against neuroblastoma cells employing significantly low doses

(2 $\mu\text{g mL}^{-1}$). This strategy can be easily adapted for the treatment of different malignancies thanks to the high versatility of the nanocarriers which compose these nanoassemblies, in addition to the high number of possible combinations that can be delivered, which would pave the way for the creation of more efficient therapies.

4. Experimental Section

Materials: The following compounds were purchased from Sigma–Aldrich Inc.: aminopropyltriethoxysilane (APTES), ammonium nitrate, cetyltrimethylammonium bromide (CTAB), tetraethyl orthosilicate (TEOS), *N*-Hydroxysulfosuccinimide sodium salt (Sulfo-NHS), *N*-(3-Dimethylaminopropyl)-*N'*-ethylcarbodiimide hydrochloride (EDC), *N,N*-diisopropylethylamine (DIPEA), fluorescein isothiocyanate (FITC), succinic anhydride, trifluoroacetic acid (TFA), *N,N*-bis(tert-butylloxycarbonyl) guanidine, (3-aminophenyl)methanol, triphenylphosphine (TPP), diisopropyl azodicarboxylate (DIAD), cholesterol, acrylamide, 2-aminoethyl methacrylate hydrochloride, *N,N'*-methylenebis(acrylamide) (MBA), ammonium persulfate (APS), *N,N,N',N'*-Tetramethylethylenediamine (TMEDA), doxorubicin hydrochloride, and AmiconUltra-2 mL Centrifugal Filters Ultracel-50K (Millipore). Lipids for the liposomes synthesis were purchased from Avanti Polar Lipids: 3-distearoyl-sn-glycero-3-phosphocholine (DSPC), 1,2-distearoyl-sn-glycero-3-phosphoethanolamine-*N*-[amino(polyethylene glycol)-2000] (ammonium salt) (DSPEPEG(2000)-NH₂), and 1,2-distearoyl-sn-glycero-3-phosphoethanolamine-*N*-[carboxy(polyethylene glycol)-2000] (ammonium salt) (DSPE-PEG(2000)-COOH). All other chemicals [absolute ethanol, *N,N*-dimethylformamide (DMF), dimethyl sulfoxide (DMSO), acetone, ethyl ether, dichloromethane (DCM), heptane, dry solvents etc.] were commercially available and of best quality and they were employed as received.

Instrumental Section: The hydrodynamic size of mesoporous nanoparticles, liposomes, protocells, and protein nanocapsules was measured by DLS employing a DynaPro MS/X, Wyatt Inc. equipment. The size of these nanoparticles was also determined by Transmission Electron Microscopy (TEM) which were carried out with a JEOL JEM 1400 instrument operated at 100 kV, equipped with a CCD camera. Sample preparation was performed by dispersing the respective nanoparticle in pure ethanol or in distilled water, depending on the sample, and subsequent deposition onto holey carbon coated copper grids. A solution of 1% of phosphotungstic acid (PTA) pH 7.0 was employed as staining agent to visualize the lipid coating of protocells or the protein capsules alone and attached on the protocell surface. Fluorescence microscopy was carried out employing a Fluorescence microscope Leica DML with digital image capture and flow cytometry was performed in a Flow cytometer, FACS Canto II for 6 fluorescence.

Synthesis of Mesoporous Silica Nanoparticles (MSNs): 1.5 μL of APTES was functionalized with 1 mg of FITC in 1 mL of EtOH (Solution A). The solution was stirred for 2 h under magnetic stirring at room temperature. Parallely, 0.290 g of CTAB was dissolved in 150 g of NH₄OH 3 M and the solution was magnetically stirred for 1 h in a 200 mL beaker sealed with parafilm (Solution B). After this time, 3 mL of TEOS 0.88 M in ethanol was added to Solution A and the resulting mixture was transferred to Solution B and the parafilm cover was removed. The reaction was maintained at 50 °C overnight under static conditions. Finally, the solution was transferred to a closed bottle and then, it was placed in an oven at 70 °C overnight. The nanoparticles were collected by centrifugation and washed with ethanol. The surfactant of the silica channels was removed by cationic extraction in a solution of 95% ethanol, 5% water, and 10 g of NH₄NO₃ mL⁻¹ at 80 °C during 3 h with reflux and under stirring. This process was repeated three times to ensure the complete surfactant elimination. The nanoparticles were washed with ethanol and finally stored in pure ethanol.

Doxorubicin Loading in MSNs: A solution of 0.5 mg of doxorubicin hydrochloride in pure water was added to an aqueous suspension of

2.5 mg of MSN with a total volume of 500 μL of water. The mixture was stirred in an orbital shaker for 24 h at room temperature. After this time, Dox-loaded MSN were collected by centrifugation and the supernatant was stored for the determination of the resulting Dox concentration after the loading step. The amount of Dox loaded in MSN was determined by the difference in absorbance of the initial Dox solution and the resulting supernatant absorbance at 490 nm.

Synthesis of Liposomes: DSPC, cholesterol, and DSPE-PEG(2000)-COOH or DSPE-PEG(2000)-NH₂, depending on the functional groups required for the liposome surface, were dissolved in chloroform with the following mol% ratios 65:20:15, respectively. The lipids were dried under vacuum, and the thin lipids film were rehydrated with 2 mL of PBS (IX). The solution was sonicated for 1 h to yield the liposome solution. Finally, liposomes were extruded 20 times using 0.1 μm polycarbonate filter membrane to obtain monodisperse liposomes solutions.

Synthesis of Protocells PC-NH₂ and PC-COOH: MSN was transferred from the ethanolic suspension to water at 2.5 mg mL⁻¹ by centrifugation (15 000 rpm, 10 min) and resuspension in water. A suspension of the corresponding liposomes 8×10^{-6} mol in 1.2 mL of PBS was added to MSN suspension and the mixture was sonicated during 20 s. After this time, the excess of liposomes was removed by centrifugation (15 000 rpm, 10 min). The pelleted protocells were redispersed in PBS (IX) by sonication; this process was repeated twice. Finally, the protocells were stored in 1 mL of PBS (2.5 mg mL⁻¹). In the case of protocells loaded with Dox, MSN were previously loaded with Dox according with the method mentioned above.

Protocell Functionalization With Targeting Moieties PC-mABG and PC-pABG: The first step was the activation of the carboxylic acid of corresponding analogue which were synthesized according to the method reported elsewhere.^[4] This step was carried out dissolving 0.018 mmol of the corresponding targeting analogue in 1 mL of PBS (pH 7.2) which contained 0.063 mmol of EDC and 0.063 mmol of sulfo-NHS. The mixture was magnetically stirred for 30 min at room temperature. This solution was added to 2.5 mg of PC-NH₂ and the mixture was stirred in an orbital shaker for 12 h. Finally, the functionalized protocells were centrifugated and resuspended in 1 mL of PBS.

Synthesis of Glucose Oxidase Nanocapsules (Gox_{nc}): First, the reaction buffer NaHCO₃ (0.01 M, pH 8.5) was deoxygenated by freeze-vacuum-N₂ cycles. 5 mg of Glucose Oxidase was dissolved in 2 mL of freshly deoxygenated buffer NaHCO₃ (pH 8.5, 0.01 M) with 10 μL of *N*-acryloxysuccinimide (12 mg mL⁻¹ in DMSO) and the solution was orbitally stirred during 2 h. The acryloylated glucose oxidase was purified by centrifugation employing 50 kDa cutoff filters (AMICON Ultra-2 mL 50 kDa) resulting in the solution A. In a separated vial, 1.71 mg of acrylamide (AA), 2.98 mg of hydrochloride salt of 2-aminoethylmethacrylate (AM) monomers, and 0.308 mg of *N,N'*-methylene bisacrylamide (MBA) were dissolved in 0.4 mL freshly deoxygenated NaHCO₃ buffer, resulting in the solution B. Solutions A and B were mixed and stirred in an orbital shaker during 10 min, resulting in solution C. Then, a solution of APS (3.08 mg) and TMEDA (2.4 μL) in 1 mL of deoxygenated NaHCO₃ was added dropwise during 10 min to the solution C. Total volume in this mixture should be 5 mL. This mixture was stirred at 300 rpm for 90 min at room temperature under nitrogen atmosphere. Next, the encapsulated enzyme was purified by centrifugal separation with 50 kDa cutoff filters (AMICON Ultra-2 mL 50 kDa) and washed three times with NaHCO₃ buffer (0.01 M pH 8.5). Gox_{nc} were preserved in PBS (pH 7.2) at 4 °C.

Attachment of Gox_{nc} on Protocells (PC-Gox_{nc}): 2.5 mg of PC-COOH was suspended in 1 mL of PBS (pH 7.2) which contained 0.008 mmol of EDC and 0.008 mmol of NHS. The suspension was stirred in an orbital shaker for 30 min at room temperature. After this time, protocells were centrifugated (15 000 rpm, 10 min) and washed three times with PBS to remove the excess of reagents. Then, protocells were suspended in 1 mL of PBS (pH 7.2) and a solution of Gox_{nc} in the same buffer was added. The mixture was stirred in an orbital shaker for 12 h and then, PC-Gox_{nc} were purified by centrifugation.

PC-Gox_{nc} Functionalization With pABG Analogue: This step was carried out dissolving 0.018 mmol of pABG analogue in 1 mL of PBS (pH 7.2)

which contained 0.063 mmol of EDC and 0.063 mmol of sulfo-NHS. The mixture was magnetically stirred for 30 min at room temperature. This solution was added to 2.5 mg of PC-Gox_{nc} and the mixture was stirred in an orbital shaker for 12 h. Finally, the functionalized protocells were centrifuged and resuspended in 1 mL of PBS.

Enzymatic Activity Measurements: The enzymatic activity of all samples was evaluated by the enzymatic assay of glucose oxidase, Merk.

Evaluation of Nanoparticle Cell Uptake of PC-T and PC-Gox_{nc}-T: For this study, 90 000 NB1691 or LAN1 cell cm⁻² were seeded into each well of a 24 well plate. The cells were incubated with 200 μL of the respective protocells with their respective concentrations for 2 h at 37 °C and 5% CO₂. After this time, cells were thoroughly washed to remove the excess of nanoparticles and the cells were incubated for 24 h at 37 °C and 5% CO₂ atmospheric concentration. Cells were then washed twice with PBS and incubated at 37 °C with trypsin–ethylenediaminetetraacetic acid (EDTA) solution for cell detachment. The reaction was stopped with culture medium after 5 min, and cells were centrifuged at 1500 rpm for 10 min and resuspended in fresh medium. Flow cytometric measurements were performed at an excitation wavelength of 488 nm, and green fluorescence was measured at 530 nm. The samples were performed in triplicate, and 20 000 cells were evaluated per sample. To calculate the percent of positive fluorescence cells, it was set a gate which contained 0.1% of control cells, and it was applied to all other samples.

Cell Viability Studies: The cytotoxic capacity of these nanocarriers was evaluated employing in vitro cellular cultures of neuroblastoma cells NB1691 and human MSC. Briefly, 90 000 NB1691 or MSC cell cm⁻² were seeded into each well of a 24 well plate. The cells were incubated with 200 μL of the respective nanocarrier concentration during 24 h at 37 °C at 5% CO₂ atmospheric concentration. Then, the supernatant was removed, and the cells were washed two times with PBS (1×) to remove the non-internalized nanocarriers. Finally, cells were harvested, and cell viability was determined by flow cytometry with 7AAD (Biolegends, San Diego, CA.) using the FACSCanto II flow cytometer and the FACSDiva software v6.1.2 (BD Biosciences, San Jose, Ca.).

In the case of the comparative cytotoxicity between neuroblastoma and healthy cells, the cells were incubated with a fixed concentration of PC-Dox-Gox_{nc}-T (70 μg mL⁻¹) during 2 hours at 37 °C at 5% CO₂ atmospheric concentration. Then, cells were thoroughly washed with PBS to remove the excess of nanoparticles and they were incubated 24 h at 37 °C at 5% CO₂ atmospheric concentration. After this time, cells were harvested, and cell viability was determined following the same protocol mentioned above.

Nanoparticle Uptake Studies by Fluorescence Microscopy and Confocal Fluorescence Microscopy: 90 000 NB1691 or human MSC cell cm⁻² were seeded into each well of a 24 well plate. The cells were incubated with 200 μL of PC-Dox-Gox_{nc}-T (70 μg mL⁻¹) during 2 h at 37 °C at 5% CO₂ atmospheric concentration. Then, cells were thoroughly washed with PBS to remove the excess of nanoparticles and they were incubated 24 h at 37 °C at 5% CO₂ atmospheric concentration. Fluorescence microscopic images were taken to evaluate nanoparticle uptake. Green channel was used to locate the fluorescein-labeled silica core and red channel was employed to visualize Dox. To determine the localization of the nanoparticle within the tumoral cell, 50 000 NB1691 cell cm⁻² were seeded into each well of a 8 well plate. Protocells functionalized with p-ABG (PC-pABG) were incubated (300 μL of 40 μg mL⁻¹) with a neuroblastoma line (NB1691) for 24 h at 37 °C at 5% CO₂ atmospheric concentration. The next day, in order to avoid cell detaching from the wall, the fixation protocol was carried out without withdrawing treatment medium. The cells were fixated with a solution of formaldehyde (4%) during 15 min. After that, the volume of each well was vacuumed, and cells were washed two times with water milli-Q. DAPI and HCS CellMask Deep Red Stain were added to label cell nuclei and cytoplasm, respectively. In this case, images were acquired with a SP8-Stellaris (Leica Microsystems) using a 63× HCX PLAPO 1.4 N.A. oil immersion objective. Acquisition software was LASX v4.5 (Leica Microsystems). Orthogonal sections and videos were done by using the same software.

Supporting Information

Supporting Information is available from the Wiley Online Library or from the author.

Acknowledgements

The present work was supported by the Spanish government by Ministerio de Ciencia e Innovación, Agencia Estatal de Investigación, project PID2019-106381RB-I00/AEI/10.13039/501100011033 and by ISCIII, Acción Estratégica en Salud, project P119/01758. J.P.N. and M.R. were supported by Asociación Pablo Ugarte. M.R. was supported by Asociación NEN and Fundación Neuroblastoma. The authors are also thankful to the National Electron Microscopy Center, UCM, and Servicio de Interacciones Moleculares of the Centro de Investigaciones Biológicas Margarita Salas, C.S.I.C. for the support with the characterization techniques, TEM and DLS.

Conflict of Interest

The authors declare no conflict of interest.

Author Contributions

The manuscript was written through contributions of all authors. All authors have given approval to the final version of the manuscript.

Data Availability Statement

The data that support the findings of this study are available in the supplementary material of this article.

Keywords

enzyme nanocapsules, nanomedicine, neuroblastoma, protocells

Received: June 17, 2022

Revised: July 29, 2022

Published online:

- [1] E. A. Newman, S. Abdessalam, J. H. Aldrink, M. Austin, T. E. Heaton, J. Bruny, P. Ehrlich, R. Dasgupta, R. M. Baertschiger, T. B. Lautz, D. S. Rhee, M. R. Langham, M. M. Malek, R. L. Meyers, J. D. Nathan, B. R. Weil, S. Polites, M. B. Madonna, *J. Pediatr. Surg.* **2019**, *54*, 383.
- [2] V. Smith, J. Foster, *Children* **2018**, *5*, 114.
- [3] L. Amoroso, R. Haupt, A. Garaventa, M. Ponzoni, *Expert Opin. Invest. Drugs* **2017**, *26*, 1281.
- [4] M. Germain, F. Caputo, S. Metcalfe, G. Tosi, K. Spring, A. K. O. Åslund, A. Pottier, R. Schifflers, A. Ceccaldi, R. Schmid, *J. Controlled Release* **2020**, *326*, 164.
- [5] Y. Xiao, T. Zhang, X. Ma, Q. C. Yang, L. L. Yang, S. C. Yang, M. Liang, Z. Xu, Z. J. Sun, *Adv. Sci.* **2021**, *8*, 2101840.
- [6] Z. Liang, Y. Tu, F. Peng, *Adv. Healthcare Mater.* **2021**, *10*, 2100720.
- [7] Y. Shi, R. Van Der Meel, X. Chen, T. Lammers, *Theranostics* **2020**, *10*, 7921.
- [8] K. Park, *J. Controlled Release* **2019**, *305*, 221.

- [9] T. Ojha, V. Pathak, Y. Shi, W. E. Hennink, C. T. W. Moonen, G. Storm, F. Kiessling, T. Lammers, *Adv. Drug Delivery Rev.* **2017**, *119*, 44.
- [10] Y. Nakamura, A. i Mochida, P. L. Choyke, H. Kobayashi, *Bioconjugate Chem.* **2016**, *27*, 2225.
- [11] S. Wilhelm, A. J. Tavares, Q. Dai, S. Ohta, J. Audet, H. F. Dvorak, W. C. W. Chan, *Nat. Rev. Mater.* **2016**, *1*, 16014.
- [12] A. K. Pearce, R. K. O'Reilly, *Bioconjugate Chem.* **2019**, *30*, 2300.
- [13] G. Villaverde, A. Baeza, G. J. Melen, A. Alfranca, M. Ramirez, M. Vallet-Regí, *J. Mater. Chem. B* **2015**, *3*, 4831.
- [14] G. Villaverde, A. Alfranca, Á. F. González Murillo, G. J. Melen, R. R. Castillo, M. Ramírez, A. Baeza, M. A. Valletá Regí, *Angew. Chem., Int. Ed.* **2019**, *58*, 3067.
- [15] K. K. Matthay, R. E. George, A. L. Yu, *Clin. Cancer Res.* **2012**, *18*, 2740.
- [16] K. Bukowski, M. Kciuk, R. Kontek, *Int. J. Mol. Sci.* **2020**, *21*, 3233.
- [17] M. Ye, Y. Han, J. Tang, Y. Piao, X. Liu, Z. Zhou, J. Gao, J. Rao, Y. Shen, *Adv. Mater.* **2017**, *29*, 1702342.
- [18] P. N. Durfee, Y.-S. Lin, D. R. Dunphy, A. J. Muñoz, K. S. Butler, K. R. Humphrey, A. J. Lokke, J. O. Agola, S. S. Chou, I.-M. Chen, W. Wharton, J. L. Townson, C. L. Willman, C. J. Brinker, *ACS Nano* **2016**, *10*, 8325.
- [19] K. S. Butler, P. N. Durfee, C. Theron, C. E. Ashley, E. C. Carnes, C. J. Brinker, *Small* **2016**, *12*, 2173.
- [20] C. E. Ashley, E. C. Carnes, K. E. Epler, D. P. Padilla, G. K. Phillips, R. E. Castillo, D. C. Wilkinson, B. S. Wilkinson, C. A. Burgard, R. M. Kalinich, J. L. Townson, B. Chackerian, C. L. Willman, D. S. Peabody, W. Wharton, C. J. Brinker, *ACS Nano* **2012**, *6*, 2174.
- [21] M. A. R. O. Villegas, A. Baeza, A. Nouredine, P. N. Durfee, K. S. Butler, J. O. Agola, C. J. Brinker, M. A. Vallet-Regí, *Chem. Mater.* **2018**, *30*, 112.
- [22] L. H. Fu, C. Qi, Y. R. u Hu, J. Lin, P. Huang, *Adv. Mater.* **2019**, *31*, 1808325.
- [23] J. Simmchen, A. Baeza, D. Ruiz-Molina, M. Vallet-Regí, *Nanoscale* **2014**, *6*, 8907.
- [24] M. R. Villegas, A. Baeza, M. Vallet-Regí, *ACS Appl. Mater. Interfaces* **2015**, *7*, 24075.
- [25] Y. Alyassin, E. G. Sayed, P. Mehta, K. Ruparelia, M. S. Arshad, M. Rasekh, J. Shepherd, I. Kucuk, P. B. Wilson, N. Singh, M.-W. Chang, D. G. Fatouros, Z. Ahmad, *Drug Discovery Today* **2020**, *25*, 1513.
- [26] G. Bozzuto, A. Molinari, *Int. J. Nanomed.* **2015**, *10*, 975.
- [27] S. P. Mornet, O. Lambert, E. Duguet, A. Brisson, *Nano Lett.* **2005**, *5*, 281.
- [28] J. S. Suk, Q. Xu, N. Kim, J. Hanes, L. M. Ensign, *Adv. Drug Delivery Rev.* **2016**, *99*, 28.
- [29] Y.-S. Lin, K. R. Hurley, C. L. Haynes, *J. Phys. Chem. Lett.* **2012**, *3*, 364.
- [30] S. N. Dean, K. B. Turner, I. L. Medintz, S. A. Walper, *Ther. Delivery* **2017**, *8*, 577.
- [31] M. A. R. O. Villegas, A. Baeza, M. A. Vallet-Regí, *Molecules* **2018**, *23*, 1008.
- [32] Y. Hui, X. Yi, F. Hou, D. Wibowo, F. Zhang, D. Zhao, H. Gao, C.-X. Zhao, *ACS Nano* **2019**, *13*, 7410.
- [33] M. Yan, J. Du, Z. Gu, M. Liang, Y. Hu, W. Zhang, S. Priceman, L. Wu, Z. H. Zhou, Z. Liu, T. Segura, Yi Tang, Y. Lu, *Nat. Nanotechnol.* **2010**, *5*, 48.
- [34] A. Baeza, E. Guisasola, A. Torres-Pardo, J. M. González-Lez-Calbet, G. J. Melen, M. Ramirez, M. Vallet-Regí, *Adv. Funct. Mater.* **2014**, *24*, 4625.
- [35] M. R. O. Villegas, A. Baeza, A. Usategui, P. L. Ortiz-Romero, J. L. Pablos, M. A. Vallet-Regí, *Acta Biomater.* **2018**, *74*, 430.
- [36] S. Rivankar, *J. Cancer Res. Ther.* **2014**, *10*, 853.
- [37] H. Tang, W. Zhao, J. Yu, Y. Li, C. Zhao, *Molecules* **2018**, *24*, 4.
- [38] S. Shah, A. Chandra, A. Kaur, N. Sabnis, A. Lacko, Z. Gryczynski, R. Fudala, I. Gryczynski, *J. Photochem. Photobiol., B* **2017**, *170*, 65.